JOURNAL OF PHYSICAL ORGANIC CHEMISTRY
J. Phys. Org. Chem. 2007; **20:** 395–409
Published online 4 April 2007 in Wiley InterScience
(www.interscience.wiley.com) DOI: 10.1002/poc.1159

Electronic and structural properties of biazulene, terazulene, and polyazulene isomers†

Jerry Ray Dias*

Department of Chemistry, University of Missouri, Kansas City, MO 64110-2499, USA

Received 10 October 2006; revised 5 January 2007; accepted 6 January 2007

ABSTRACT: Facile graph theoretical MO solutions are demonstrated. The dihedral angles between the azulene units at the bridging bond in biazulenes were determined by MM2 calculations. Polyazulenes are predicted to be conductive only via the polaron mechanism. Polaron conduction in 1,3- and 2,6-polyazulene is qualitatively predicted to be more facile than in 4,8- and 5,7-polyazulene. Copyright © 2007 John Wiley & Sons, Ltd.

KEYWORDS: biazulene; polaron conduction; molecular orbital calculations

INTRODUCTION

Azulene ($C_{10}H_8$) is probably the smallest isolable organic compound having an intense color (blue). Naphthalene, its closest isomer, is colorless. This fact alone is responsible for the considerable interest in azulene.[1] Also, azulene is a nonalternant hydrocarbon (nonAH) and naphthalene is an alternant hydrocarbon (AH). AHs have no odd size rings and obey the pairing theorem, whereas nonAHs do not obey the pairing theorem and are invariably more polar than their AH isomers.[2] The Ullmann reaction has been used to synthesize 2,2'-biazulene and related isomers.[3] HMO calculations have also been performed on 2,2'-, 4,4'-, and 5,5'-biazulene.[4] Treatment of a 4:1 mixture of 1-bromo- and 1,3-dibromoazulene with $NiBr_2(Ph_3P)_2$, Zn, and Et_4NI gave biazulene, terazulene, and quarterazulene; reductive coupling of 1,3-dibromoazulene gave polyazulene.[5] Thus intensely colored 1,3-polyazulene oligomers (Fig. 1) have been synthesized. The synthesis of 1,3-polyazulene was accomplished by reacting 1,3-dibromoazulene with $Ni(COD)_2$ and was characterized as having an average molecular weight corresponding to 130 azulene units.[6] The ^1H NMR and FT-IR spectra of 1,3-polyazulene show signals similar to azulene. 1,3-Polyazulene was made significantly conductive by exposure to iodine or trifluoroacetic acid vapor for several days. Protonation of 1,3-polyazulene by trifluoroacetic acid followed by oxidation was found to exhibit high conductivity and paramagnetic properties via formation of cation radicals (polarons). The electronic structure of 1,3-polyazulene has been studied by the SCF method for both its neutral and oxidized states.[7] These calculations suggested that positive net charges of the oxidized states are mainly localized in the seven membered rings and that in the polaron state the charge and spin parts are in separate rings of azulene unit. While 1,3-polyazulene has been extensively studied, the remaining symmetrical polyazulene polymers have not yet been considered (Fig. 1).

The current objective is to study the relative electronic properties of symmetrical biazulene and polyazulene isomers. Using graph theoretical methods, the electronic properties of polyazulenes presumed to have coplanarity between their azulene units are first computed. Then the dihedral angles between the two bridging azulene units of the biazulene isomers are determined by MM2 calculations. These dihedral angles are used to model noncoplanarity of the various polyazulene isomers. The electronic properties of the polyazulenes in which the azulene units are coplanar versus those having their azulene units uniformly twisted are compared.

RESULTS AND DISCUSSION

Facile calculation of the molecular orbitals (MOs) of azulene

The eigenvalues (energy levels) of azulene are given in Fig. 2 which shows the antisymmetric (right-hand mirror-plane fragmentation)[8] and symmetric eigenvalues (deduced from the algorithmic application of this equation: $-XC_{iu} + C_{ir} + C_{is} + C_{it} = 0$ per Fig. 3).[9] From the results in Fig. 2, it is apparent that the irreducible substructure

**Correspondence to:* J. R. Dias, Department of Chemistry, University of Missouri, Kansas City, MO 64110-2499, USA.
E-mail: diasj@umkc.edu
†Dedicated to Dr Edward C. Kirby on the occasion of his 70th birthday.

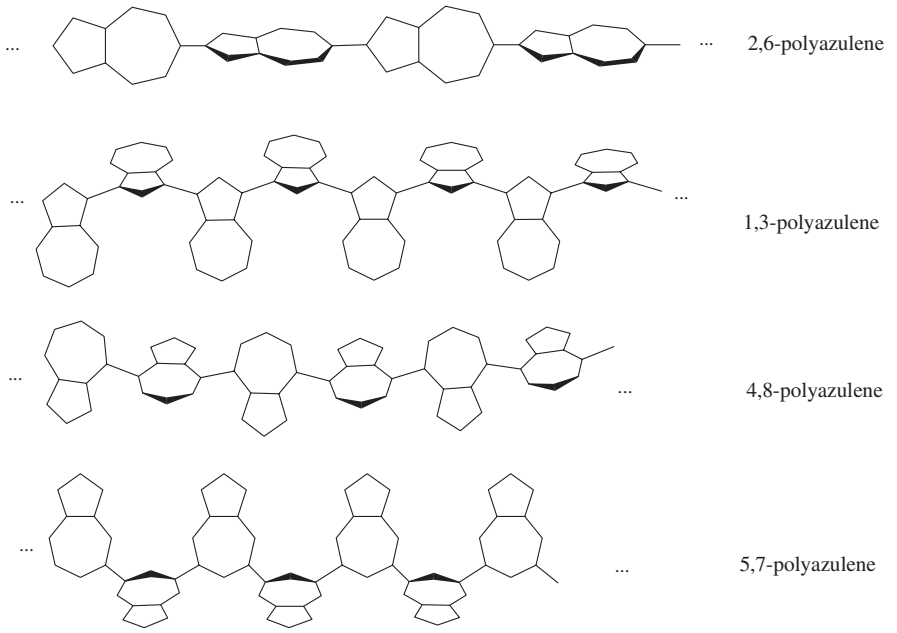

Figure 1. Polyazulene polymers in a linear staggered conformation

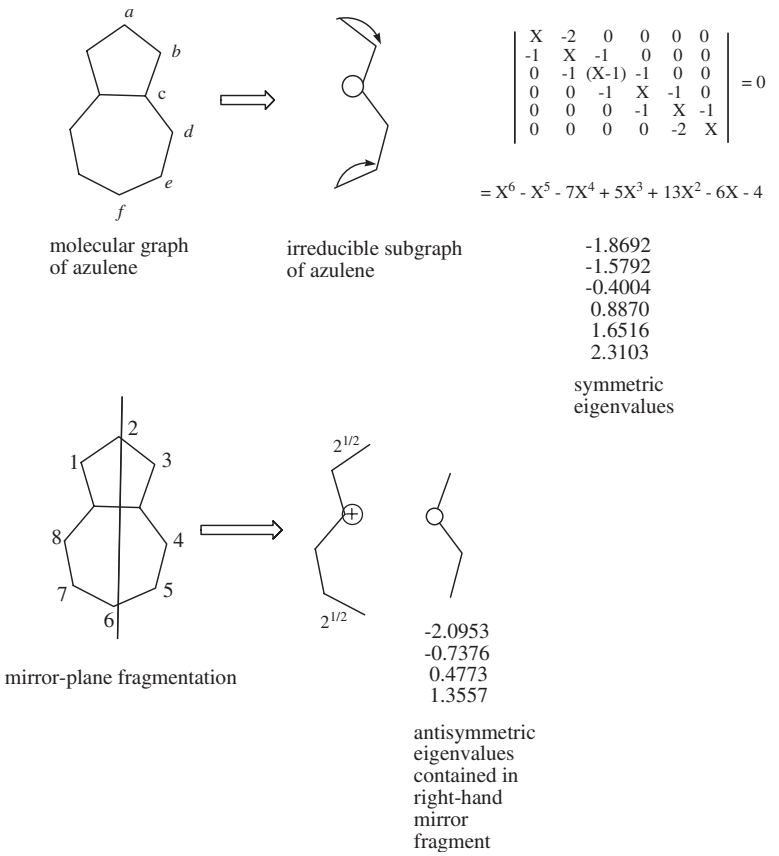

Figure 2. The irreducible subgraph and the lefthand mirror-plane fragment of azulene are identical

determined for symmetrical eigenvectors and the left-hand mirror-plane fragment both give the same eigenvalue set. Here it is important to note that the number of eigenvalues in the right-hand fragment (McClelland subgraph) is equal to the number of antisymmetric eigenvalues. Both mirror-plane fragmentation and the equation in Fig. 3 lead to computational simplification by exploiting the C_{2v} symmetry of the azulene unit in polyazulene.

DOI: 10.1002/poc

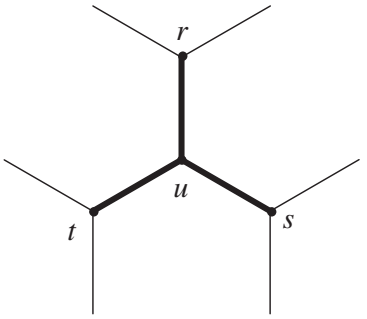

general vertex u

$$-X_iC_{iu} + C_{ir} + C_{is} + C_{it} = 0$$

Figure 3. The general relationship for any given molecular graph vertex u and its eigenvector coefficient C_{iu} for any ith eigenvalue X_i belonging to the molecular graph

Facile molecular orbital (MO) solution of conjugated polymers

The methodology used for solution of azulene above (Fig. 2) will be employed in the determination of the symmetrical eigenvalues for conjugated polymers. The recursive application of the above equation (Fig. 3) on the monomeric unit of conjugated polymers was shown to coincide with the density of states as determined via the method of Hosoya and coworkers.[9,10] In this paper, Hosoya and coworkers noted that because of a theorem which states that the density of states is independent of the boundary condition,[11] it is standard practice to use cyclic boundary conditions for the analysis of linear polymer systems. These workers demonstrated that the presence of a zero HOMO – LUMO band gap in certain classes of polymer networks is predicted by the existence of non-bonding MO (NBMO) in their hypothetical cyclic monomer ($k = 0$) or dimer ($k = 0$, 1), with the cyclic monomer being equivalent to the Hückel cyclic unit and the cyclic dimer being equivalent to the Möbius cyclic unit.[12] While the eigenvalues of the Hückel cyclic monomer ($k = 0$) are present in all cyclic sizes and thus the infinite cyclic polymer strip, the eigenvalues of the Möbius cyclic unit corresponds to the Hückel cyclic dimer ($k = 0$, 1) exclusive of the eigenvalues for $k = 0$ and are present in the cyclic dimer ($2k\pi/n = 2\pi/2 = \pi$), all even cyclic units, and the infinite cyclic polymer strip $2k\pi/n = 2(\infty - 1)\pi/\infty = \pi$]. It was shown that recursive application of the equation in Fig. 3

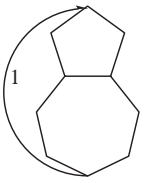

$$X^{10} - 12X^8 + 48X^6 - 2X^5 - 78X^4 + 2X^3 + 50X^2 + 2X - 9 = 0$$

−2.2308	0.4773
−2.0953	1.2131
−1.2766	1.3557
−0.7376	1.5073
−0.6960	2.4831

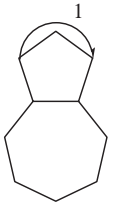

$$X^{10} - 12X^8 - 2X^7 + 46X^6 + 12X^5 - 67X^4 - 22X^3 + 32X^2 + 12X = 0$$

−2.3028	0.0
−1.8231	1.0
−1.1976	1.3028
−1.0	1.7825
−0.3910	2.6291

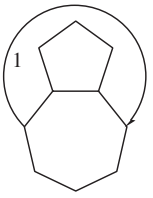

$$X^{10} - 12X^8 + 46X^6 - 4X^5 - 68X^4 + 16X^3 + 33X^2 - 12X = 0$$

−2.41421	0.41421
−1.73205	1.0
−1.5616	1.0
−1.0	1.73205
0.0	2.5616

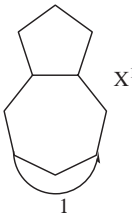

$$X^{10} - 12X^8 - 2X^7 + 48X^6 + 12X^5 - 75X^4 - 16X^3 + 43X^2 + 4X - 4 = 0$$

−2.1935	0.2950
−1.7203	0.9239
−1.3308	1.1935
−1.2950	2.0
−0.3775	2.5047

Figure 4. Hückel cyclic monomers ($k = 0$) of 2,6-, 1,3-, 4,8-, and 5,7-polyazulenes and their characteristic polynomials where looped bond has a weight of 1

DOI: 10.1002/poc

gives the symmetric eigenvalues characteristic to the Hückel (monomer, $k=0$) cyclic unit,[9] and herein it will be shown that this equation can also be adapted to give the symmetric eigenvalues characteristic of the Möbius (dimer, $k=1$) cyclic unit.

Facile solution of the cyclic monomer and dimer of various polyazulenes

The characteristic polynomials for the Hückel cyclic monomer ($k=0$) and the Möbius cyclic monomer ($k=1$) for the polyazulenes in Fig. 1 are given in Figures 4 and 5, respectively. These characteristic polynomials and corresponding eigenvalues are for planar conformations of the polyazulens in Fig. 1. In the following, we will detail facile solutions to the symmetric and antisymmetric eigenvalues corresponding to these molecular systems. We will see that for nonAHs, the symmetric eigenvalue singular points for the density of states belonging to the band gap was given by the cyclic monomer (Hückel cyclic monomer) for infinite 1,3-, 4,8-, and 5,7-polyazulenes but for infinite 2,6-Polyazulene it was given by the cyclic dimer (Möbius cyclic monomer).

The equation in Fig. 3 will be deployed to obtain the symmetric eigenvalues for the Hückel cyclic monomers and Möbius cyclic monomers, where the latter application is new; here it needs to be stressed that the eigenvalues of the cyclic monomer ($k=0$) are present in all cyclic sizes and the eigenvalues of the Möbius cyclic monomer are the eigenvalues present in the Hückel cyclic dimer ($k=0$ and 1) exclusive of those for $k=0$. Figures 6 and 7 give all the corresponding symmetric eigenvalues for these monomers and dimers, respectively. To adapt the application of the equation in Fig. 3 to Möbius cyclic monomer systems (Fig. 5), it needs to be noted that looped bond has a negative weight, thus accounting for the minus sign for the symmetric eigenvector coefficient in Fig. 7. For Fig. 6, a number of points should be noted. First, since these eigenvalues are present in all cyclic sizes, the smallest negative eigenvalues (-0.3910, 0, and -0.3775β) in 1,3-, 4,8-, and 5,7-polyazulene (last three mers) correspond to the LUMO of these infinite (and finite) systems; these negative eigenvalues are smaller than the negative eigenvalues present in Fig. 7. Second, the repeat unit

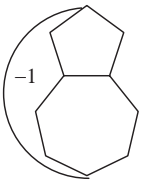

$$X^{10} - 12X^8 + 48X^6 - 2X^5 - 70X^4 + 10X^3 + 26X^2 - 6X - 1 = 0$$

−2.1068	0.4773
−2.0953	0.5273
−1.6621	1.3557
−0.7376	2.0764
−0.1144	2.2796

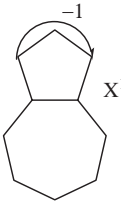

$$X^{10} - 12X^8 + 2X^7 + 50X^6 - 16X^5 - 83X^4 + 34X^3 + 44X^2 - 12X - 8 = 0$$

−2.2651	0.7429
−2.0	1.0
−1.7650	1.5223
−0.61803	1.61803
−0.4073	2.1723

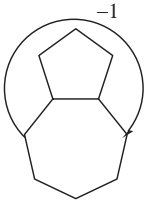

$$X^{10} - 12X^8 + 50X^6 - 84X^4 + 49X^2 - 8 = 0$$

−2.1940	0.5176
−1.9318	0.8106
−1.5940	1.5904
−0.8106	1.9318
−0.5176	2.1940

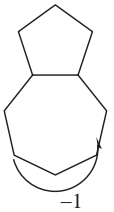

$$X^{10} - 12X^8 + 2X^7 + 48X^6 - 16X^5 - 71X^4 + 32X^3 + 27X^2 - 8X - 4 = 0$$

−2.3541	0.6938
−2.0615	0.8139
−1.6431	1.3375
−0.4194	1.7640
−0.3963	2.2653

Figure 5. Möbius cyclic monomers ($k=1$) of 2,6-, 1,3-, 4,8-, and 5,7-polyazulenes and their characteristic polynomials where the looped bond has a weight of -1

DOI: 10.1002/poc

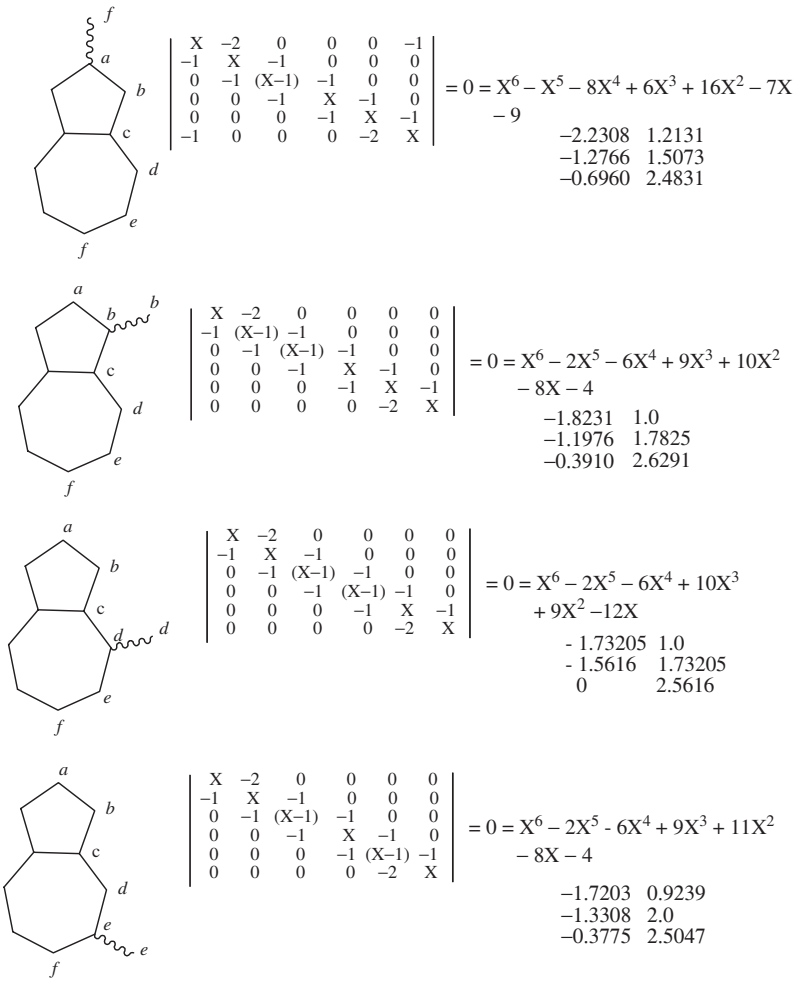

Figure 6. Solution of the Huckel ($k = 0$) repeat unit of polyazulenes recursively using the equation in Figure 3 to obtain the symmetric eigenvalues

for 4,8-polyazulene (third mer from the top in Fig. 6) has distinct paired eigenvalues of $\pm\sqrt{3}$, 1.0, and 0 β and complementary eigenvalues of $\frac{1}{2}(\sqrt{17} \pm 1)$ which are present in all cyclic sizes. Recursive application of the relationship[9] given in Fig. 3 allows us to easily obtain the corresponding eigenvectors for these eigenvalues which we will now illustrate. These eigenvalues belong to symmetrical eigenvector set. Consider the third structure in Fig. 6. Starting with the zero eigenvalue ($X = 0$), the sum of the coefficients at position a must sum to zero ($b + b = 0$) and comply with the C_2 symmetry axis which means that $b = 0$. For position b, the sum of the coefficients is $a + c = 0$ or $c = -a$. Proceeding to position c, we obtain $b + c + d = 0$ or $c = -d$ and $d = a$. Going to position d, we obtain $c + e + d = 0$ or $e = 0$, and finally for position e, we obtain $d + f = 0$ or $f = -a$. Assigning $a = 1$ gives the unnormalized eigenvector (First structure in Fig. 8) for the zero eigenvalue of 4,8-polyazulene.

Application of this recursive procedure for the eigenvalue of one ($X = 1$) in the 4,8-polyazulene mer (Fig. 6) is further illustrative, since the use of the equation in Fig. 3 will require one additional parameter. The recursive application of this equation while noting proper symmetry, one can easily determine the corresponding symmetrical eigenvector coefficients for integer and surd eigenvalues. Starting at position a, we obtain $-a + 2b = 0$ or $a = 2b$. Proceeding next to position b, we obtain $a - b + c = 0$ or $c = -b$. Going to position c, we obtain $- c + b + c + d = 0$ or $b = -d$. Operating on position d gives $- d + c + d + e = 0$ or $e = b$. Finally, operating on position e gives $- e + d + f = 0$ or $f = 2b$. Setting $b = 1$ gives the eigenvector coefficients shown in Fig. 8 (2nd structure).

The right-hand fragment (McClelland subgraph) in mirror-plane fragmentation gives the antisymmetric eigenvalues of the corresponding molecular graph. Figures 9 and 10 give the mirror-plane fragments to all the respective cyclic monomers in Figures 6 and 7 and their corresponding antisymmetric eigenvalues. The McClelland subgraphs with characteristic polynomials and corresponding eigenvalues for the Hückel

DOI: 10.1002/poc

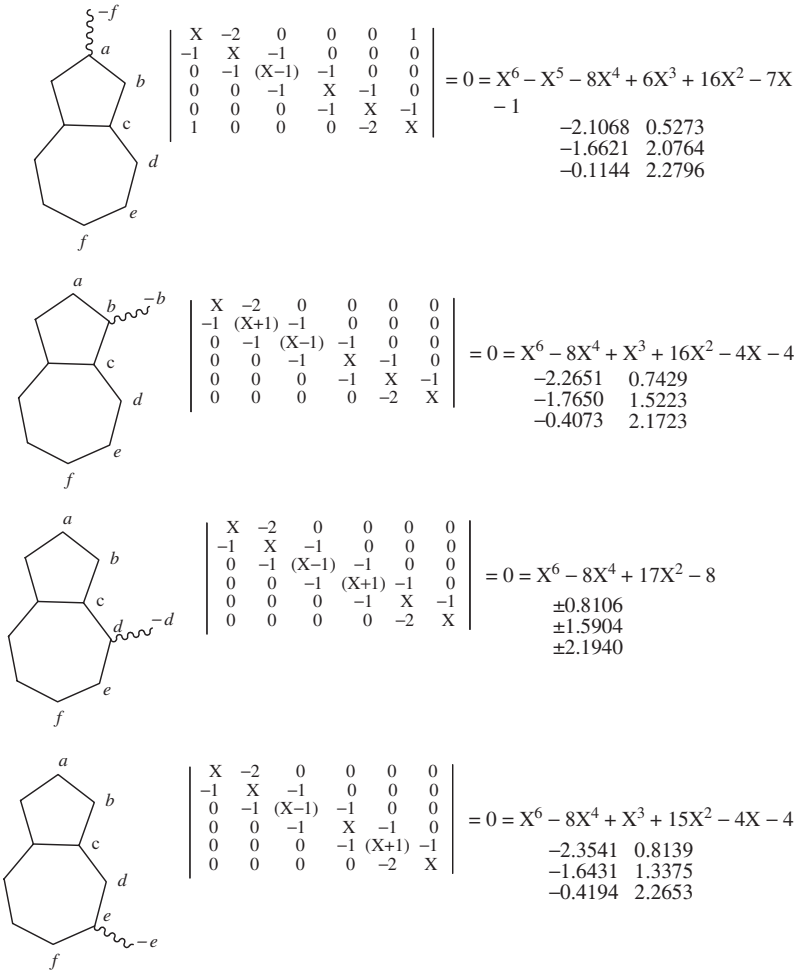

Figure 7. Solution of the Mobius ($k = 1$) repeat unit of polyazulenes recursively using the equation in Figure 3 to obtain the symmetric eigenvalues

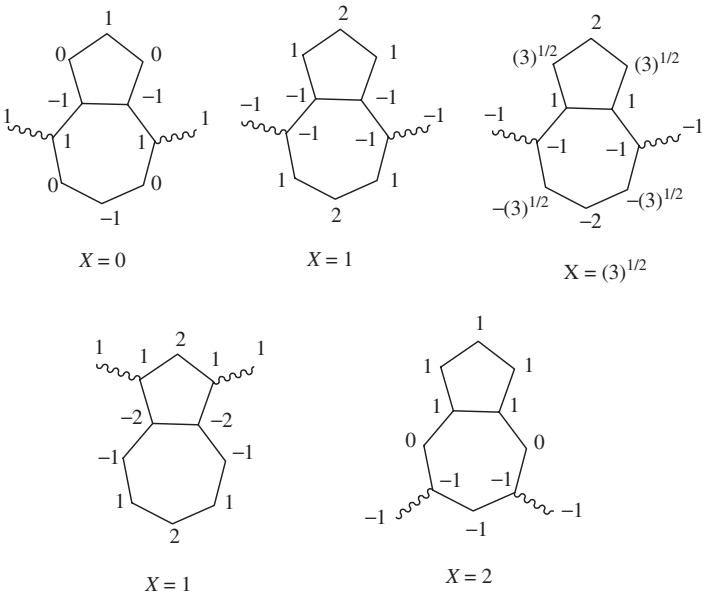

Figure 8. Select symmetric eigenvectors for 1,3-, 4,8-, and 5,7-polyazulenes computed using the relationship given in Figure 3

DOI: 10.1002/poc

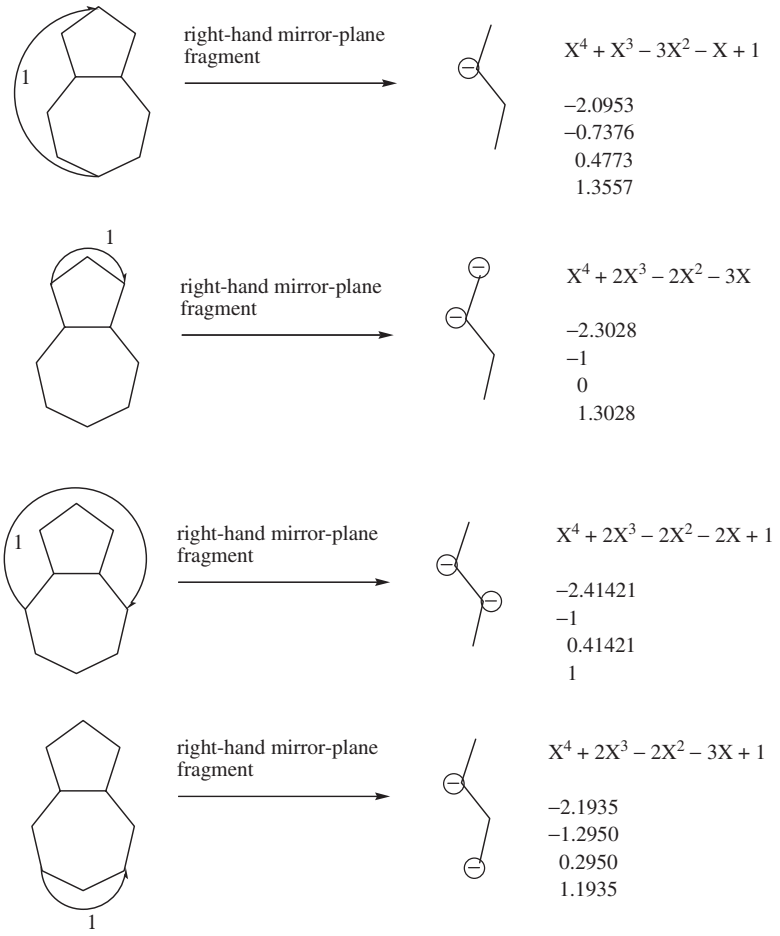

Figure 9. Right-hand mirror-plane fragments (McClelland subgraphs) for the Hückel cyclic monomers given in Figure 4

cyclic monomers in Fig. 9 can be found in Table 2.1 of reference [13]. As it is evident form the first structure in Figures 9 and 10, both the Hückel and Möbius cyclic monomers for 2,6-polyazulene have the same McClelland subgraph making the cyclic dimer doubly degenerate in these eigenvalues.

The only polyazulene in Fig. 1 that can be mirror-plane fragmented is 2,6-polyazulene (top structure). In fact, 2,6-polyazulene has multiple McClelland subgraphs, one for each mer and this subgraph is the right-hand fragment shown in Fig. 2 for azulene (-2.0953, -0.7376, 0.4773, and 1.3557β). Thus, 2,6-polyazulene is highly degenerate in these eigenvalues, and this does not change even for large dihedral angles between the mers. The bandgap for planar 2,6-polyazulene (zero dihedral angle, $\varphi = 0^\circ$ between the mers) is HOMO $-$ LUMO $= 0.4773 - (-0.1144) = 0.5917\beta$. For all the polyazyulenes in Fig. 1, it can be generalized that all the corresponding HOMOs will have antisymmetric eigenvectors and all the LUMOs will have symmetric eigenvectors. Table 1 summarizes the bandgaps for all the planar polyazulenes. 2,6-Polyazulene is most unique of the polyazulenes listed in Fig. 1 in five distinct ways. First, 2,6-polyazulene has the same HOMO ($=0.4773\beta$) regardless of its dihedral angle. Second, its bandgap is determined by its cyclic dimer (Möbius cyclic monomer) while the other polyazulenes have their bandgaps determined by their cyclic monomer (Hückel cyclic monomer). Third, for a strip with its azulene units in a coplanar conformation, its point group symmetry would be C_{2v} while the other polyazulenes would belong to the C_s point group symmetry in their planar conformations. Fourth, the polymerization axis coincides with the monomer symmetry axis. Fifth, its monomeric units have head-to-tail dipole alignments (azulene has a gas phase dipole moment of 0.8 D).

Dihedral angles in biazulene isomers

We will now determine the effect of nonplanarity of the azulene mers on eigenvalues polyazulene strips in Fig. 1. In order to model this conformational effect, the dihedral angles between neighboring azulene units in the relevant

DOI: 10.1002/poc

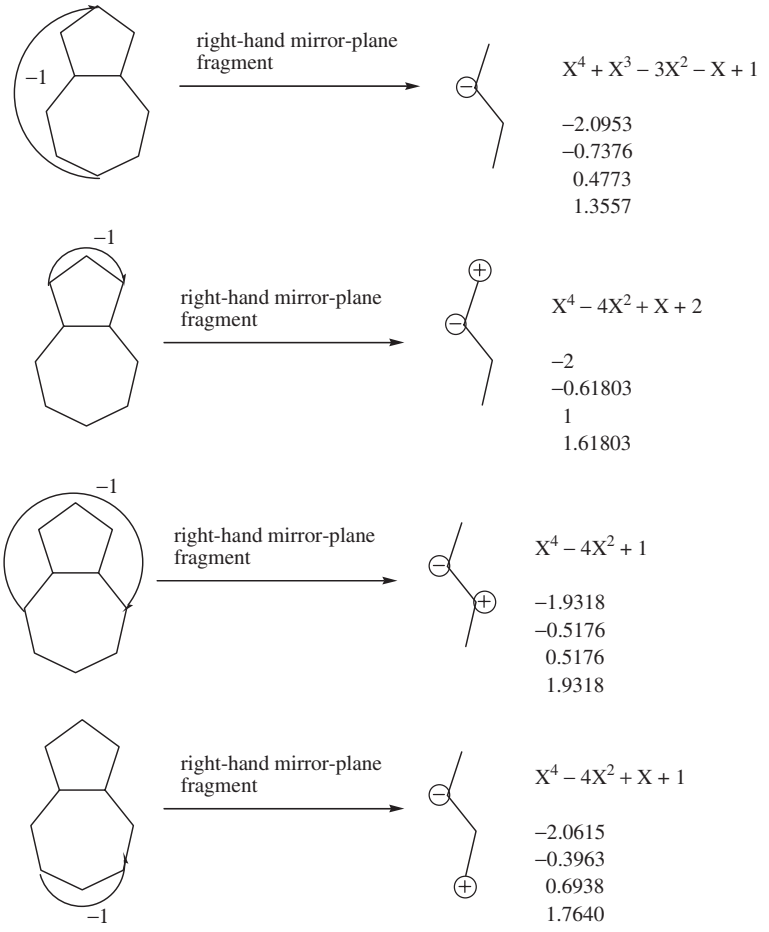

Figure 10. Right-hand mirror-plane fragments (McClelland subgraphs) for the Möbius cyclic monomers given in Figure 5

Table 1. Polyazulene HOMO – LUMO bandgaps

Polyazulene	Bandgap (β) for Dihedral Angle of 0°	Dihedral Angle, °	Bandgap (β)
2,6-	0.5917	31.45	0.6261
1,3-	0.3910	42.5	0.4919
5,7-	0.4142	54.1	0.7461
4,8-	0.6725	73.4	0.7373

isomeric biazulenes (Fig. 11) were determined via molecular mechanics (MM2). The dihedral angles for 1,3-, 2,6-, 4,8-, and 5,7-biazulene are $\varphi = 42.5°$, 31.45°, 73.4°, and 54.1°, respectively. These results are consistent with *ab initio* calculation of the dihedral angles between neighboring benzene units in biphenyl and terphenyl which ranges from 39.6°–52.2° depending on the basis set.[14] The magnitude of these angles is indicative of their relative steric/torsional strain energy. In Table 2 there is a parallelism between this steric/torsional energy for the 2,1′-, 2,5′-, and 2,4′-biazulenes where the 2-position of one azulene unit moves consecutively to the positions of 1′, 5′, and 4′ and the 1,1′-, 5,5′-, and 4,4′- biazulenes. It is seen from Table 2 that the first set of three biazulenes where the position of one azulene unit is held fixed are less sterically hindered as measured by both the corresponding smaller dihedral angle and bridging bond length than the second set of three biazulenes in which the respective positions are doubled-up. In other words, by holding the position of one azulene unit constant in the first set of biazulenes, we are probing the relative steric hindrance of positions 1, 5, and 4.

This order for the bridging bond lengths (Table 2) of the 1,1'-, 5,5'-, and 4,4'-biazulene is also consistent with the above the magnitude of the azulene HOMO normalized coefficients for position 1, 5, and 4 which are 0.5428, 0.3355, and 0.1601, that is, formation of 1,1'-biazulene from azulene involves the largest HOMO coefficient value leading to the strongest interaction and shortest bridging bond length and formation of 4,4'-biazulene involves the smallest HOMO coefficient value leading to the weakest interaction and longest bridging bond length.

Because Imamura and coworkers[14] determined that the dihedral angle for neighboring benzene rings in biphenyl to hexaphenyl were almost uniformly 39° down the chain,

DOI: 10.1002/poc

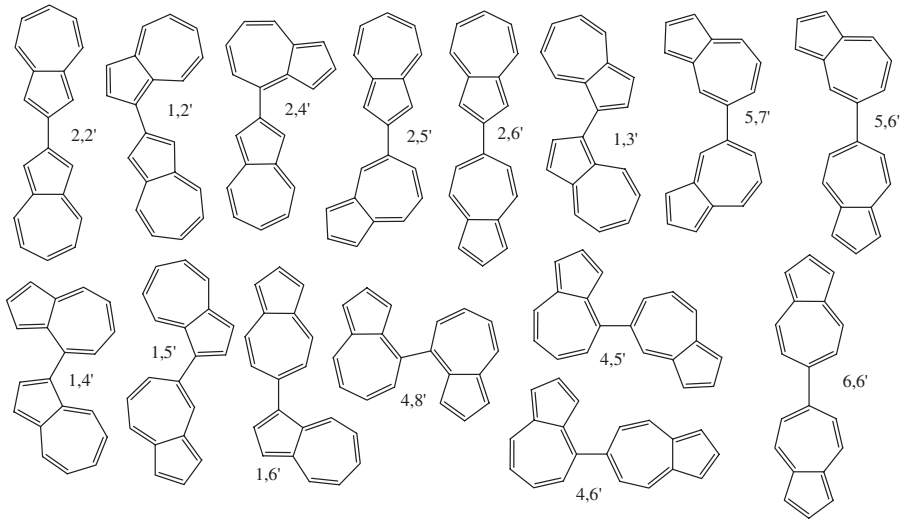

Figure 11. All possible biazulene isomers

Table 2. MM2 calculated dihedral angles and intervening bridging bond of various biazulenes

Biazulene	Dihedral Angle, °	Bridging Bond Length, Å
$1,2' = 2,1'$	38	1.469
$2,5'$	39.8	1.482
$2,4'$	49.8	1.487
$1,3' = 1,1'$	42.5	1.471
$5,7' = 5,5'$	54.1	1.503
$4,8' = 4,4'$	73.4	1.510

we now assume that the above MM2 calculated dihedral angles (also, confer with Table 1) for the biazulenes apply uniformly throughout the chains for the polyazulenes given in Fig. 1. Thus the bridging bonds in these polyazulenes are weighted according to the cosine of the corresponding dihedral angles. This assumption gives cos $90^\circ = 0$ resulting in these polyazulene chains having azulene units being in perpendicular conformations with zero orbital overlap between adjacent azulenes. The resulting orthogonal molecular orbitals produce highly degenerate eigenvalues corresponding to the eigenvalues of azulene as a logical consequence. Using cos $42.5^\circ = 0.7373$, cos $31.45^\circ = 0.8531$, cos $73.4^\circ = 0.2857$, and cos $54.1^\circ = 0.5864$ as the weights of the bridging looped bonds for the cyclic Hückel and Möbius monomers of 1,3-, 2,6-, 4,8-, and 5,7-polyazulenes, respectively, give the characteristic polynomials and corresponding eigenvalues presented in Figures 12 and 13, respectively, in analogy to Figures 4 and 5.

The bandgaps in Table 1 show that as the dihedral angle increases so do the bandgaps. The maximum dihedral angle of $\varphi = 90^\circ$ which results in perpendicular azulene monomer units will give a maximum bandgap of HOMO $-$ LUMO $= 0.8777\beta$ belonging to azulene for all the polyazulenes in Fig. 1. A major conclusion at this point is, regardless of the dihedral angle, all the polyazulenes in Fig. 1 have significant band gaps (i.e., the order of or greater than the HOMO – LUMO $= 0.4394\ \beta$ for pentacene) and therefore cannot exhibit metallic conductivity. Thus any conductivity associated with polyazulenes must derive via polymer doping and the resulting polaron mechanisms.

Polaron model for conduction in polyazulenes

According to simple band theory the continuum of occupied MOs of neutral molecules correspond to the valence band, the continuum unoccupied MOs correspond to the conduction band, and the void between these two bands represents the band gap which corresponds to the HOMO – LUMO where HOMO corresponds to the upper valence band edge (Fermi energy level) and the LUMO corresponds to the lower edge of the conduction band. A wide band gap leads to an insulator material, a narrow band gap leads to a semiconductor material because at room temperature thermal excitation of electrons from the valence band to the conduction band promotes conduction, and a zero band gap (HOMO – LUMO $= 0$) leads to high conductivity characteristic of metals because the electrons are thermally distributed at the interface between the adjacent valence band and conduction bands. Conductive polymers conduct current without having a zero band gap by mechanisms involving polarons, bipolarons, and solitons. Polarons, bipolarons, and solitons are generated in conjugated polymers by doping processes. Oxidation is called *p*-doping and reduction is called *n*-doping. In the doped form, the polymer backbone is either positively or negatively

DOI: 10.1002/poc

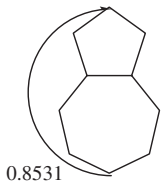

$$X^{10} - 11.728X^8 + 46.094X^6 - 2X^5 - 73.873X^4 + 2.588X^3 + 46.332X^2 + 1.4124X - 8.140 = 0$$

−2.1625	0.4773
−2.0953	1.1963
−1.3104	1.3557
−0.7376	1.4890
−0.6591	2.4452

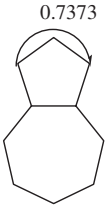

$$X^{10} - 11.544X^8 - 1.475X^7 + 43.331X^6 + 8.322X^5 - 62.712X^4 - 14.644X^3 + 30.381X^2 + 7.935X - 1.051 = 0$$

−2.2311	0.0981
−1.8274	0.9745
−1.2904	1.3116
−0.9158	1.7516
−0.3938	2.5227

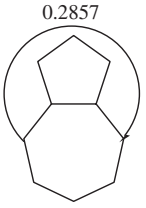

$$X^{10} - 11.082X^8 + 41.0X^6 - 2.571X^5 - 59.939X^4 + 8.449X^3 + 29.531X^2 - 4.041X - 2.857 = 0$$

−2.1671	0.4616
−1.8151	0.9159
−1.5756	1.2313
−0.8122	1.6729
−0.2757	2.3639

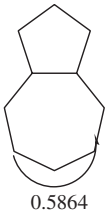

$$X^{10} - 11.344X^8 - 1.173X^7 + 43.407X^6 + 6.210X^5 - 66.299X^4 - 7.386X^3 + 37.067X^2 + 1.518X - 4.0 = 0$$

−2.1378	0.3587
−1.7490	0.9115
−1.4484	1.2424
−1.0499	1.8726
−0.3874	2.3872

Figure 12. Hückel cyclic monomers ($k = 0$) of 2,6-, 1,3-, 4,8-, and 5,7-polyazulenes and their characteristic polynomials where looped bond has the weight indicated

charged, and the small counterions derived from the dopants, such as I_3^- or Na^+, act as bystanders that do not influence the electrical properties directly.[15] Polarons are normally bound to oppositely charged counterions so that polaron conduction involves electron or hole hopping from the region of one counterion to another. This conduction is influenced by both counterion density (concentration) and mobility (temperature).

When an electron is removed from the top of the valence band of a conjugated polymer, a vacancy (hole or radical cation) is created that does not delocalize completely as expected from band theory. Only partial delocalization occurs, extending over several monomeric units causing this region to structurally deform. The energy level associated with this radical cation gives a destabilized MO thrusted into the band gap region (Fig. 14). This rise in energy is similar to the rise in energy that takes place after removal of an electron from a filled bonding MO. A radical cation that is partially delocalized over some polymer segment is called a 'polaro'. It stabilizes itself by electrostatically polarizing the medium around it. The polaron has associated with it localized electronic midgap states.

If another electron is removed from a polymer containing a polaron, either another polaron can form in a different segment of the polymer chain or a 'bipolaron' can form if the electron is removed from the vicinity an already existing polaron. Low doping levels give rise to polarons and high doping levels can produce bipolarons. The two positive charges of a bipolaron act as a pair. Both polarons and bipolarons are mobile and can move along the polymer chain by rearrangement of the double and single bonds in the conjugated system that occurs in an electric filed; the two positive charges of a bipolaron move in unison. If high doping forms a large number of bipolarons, their energies can start overlapping at the edges creating a narrow bipolaron band in the band gap region. The polaron has a spin of $\frac{1}{2}$ and the bipolaron, in compliance with the Pauli exclusion principle, has a spin of zero, that is, it is spinless. In infinite polyacetylene, which to the zero-order approximation would have a degenerate ground state, the bipolaron dissociates into two nearly independent cations because of Jahn–Teller distortion, which are also spinless and are called 'solitons'. Solitons do not form in polymers with nondegenerate ground states.

DOI: 10.1002/poc

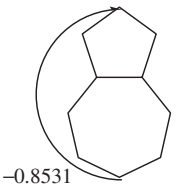

$X^{10} - 11.728X^8 + 46.095X^6 - 2X^5 - 67.049X^4 + 9.412X^3 + 25.857X^2 - 5.412X - 1.315 = 0$

–2.0953	0.4773
–2.0210	0.5670
–1.6796	1.3557
–0.7376	2.0112
–0.1488	2.2699

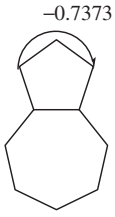

$X^{10} - 11.543X^8 + 1.475X^7 + 46.280X^6 - 12.322X^5 - 74.509X^4 + 26.644X^3 + 39.229X^2 - 9.760X - 6.949 = 0$

–2.1102	0.7816
–2.0240	0.8947
–1.7481	1.4942
–0.6404	1.5612
–0.4057	2.1966

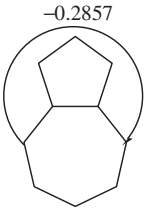

$X^{10} - 11.082X^8 + 42.143X^6 - 1.429X^5 - 64.51X^4 + 3.878X^3 + 34.102X^2 - 0.612X - 5.143 = 0$

–2.0391	0.4909
–1.9347	0.8613
–1.5833	1.4996
–0.6671	1.6306
–0.5263	2.2680

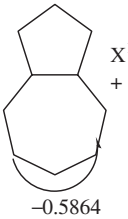

$X^{10} - 11.344X^8 + 1.173X^7 + 43.407X^6 - 10.210X^5 - 63.954X^4 + 20.761X^3 + 27.684X^2 - 5.518X - 4.0 = 0$

–2.1253	0.6111
–2.0694	0.8499
–1.6296	1.4508
–0.5077	1.5542
–0.4120	2.2780

Figure 13. Möbius cyclic monomers ($k = 1$) of 2,6-, 1,3-, 4,8-, and 5,7-polyazulenes and their characteristic polynomials where the looped bond has the weight inicated

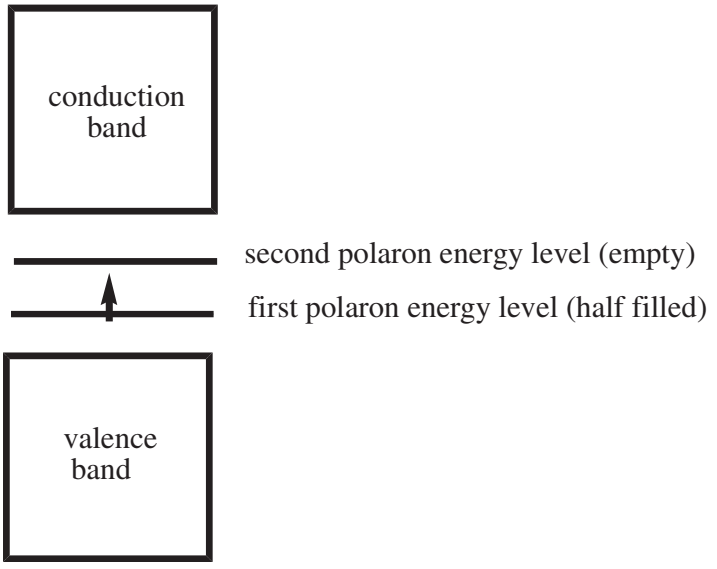

Figure 14. Polaron energy levels relative to the conduction and valence bands generated via oxidative doping

DOI: 10.1002/poc

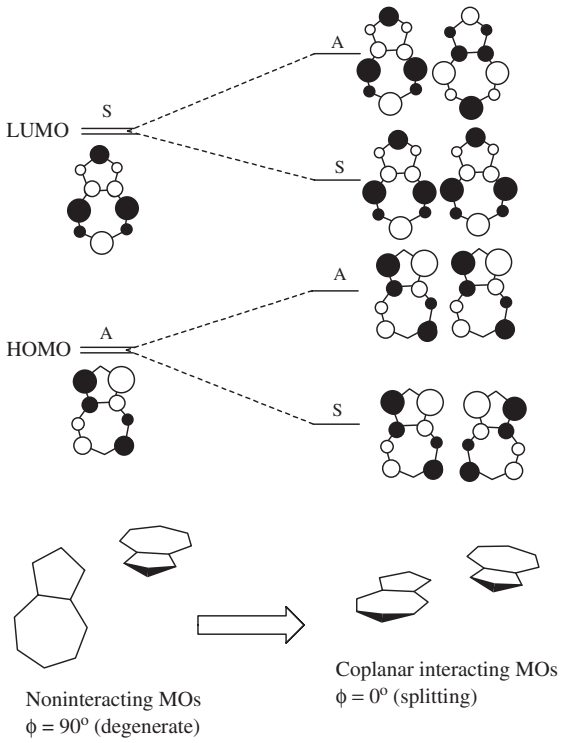

Figure 15. Construction of HOMO – LUMO energy level diagram for biazulene. The bottom part of the figure shows two azulene molecules perpendicular to each other ($\phi = 90^\circ$) and thus noninteracting. Their separate MOs are degenerate. When the dihedral angle ϕ is allowed to decrease to 0°, the azulene MOs interact and splitting occurs as shown in the upper right-hand part of the figure

The energy diagram for the construction of the HOMO – LUMO for biazulene from a degenerate pair of azulenes is shown in Fig. 15. If the pair of bonded azulenes are oriented perpendicularly (dihedral angle, $\varphi = 90^\circ$) to each other, their individual MOs are noninteracting and are simply equal to the degenerate MOs of the azulenes. When this pair of azulenes are made coplanar (dihedral angle, $\varphi = 0^\circ$), their MOs interact according to the magnitude of the coefficients in corresponding MOs of the azulene units (Fig. 16) resulting in their splitting in accordance to the Jahn–Teller theorem. For neutral biazulene this splitting to the first approximation leads to little change in overall energy because the destabilization energy of the higher antisymmetric (A) MO is almost cancelled out by the stabilization energy of the lower symmetric (S) MO. However, removal of an electron to form a polaron from the A MO does lead to more substantial stabilization due to splitting. Thus, in the absence of severe steric repulsion, coplanarity ($\varphi = 0^\circ$) should be favored by ionization. When an electron is removed from the top of the valence band of a conjugated polymer creating a polaron, only partial delocalization over several monomeric units occurs causing them to deform structurally and form a localized electronic midgap states (Fig. 14). This same model was proposed by Imamura and coworkers for biphenyl.[14]

Figures 17–20 shows what happens to the MOs in the conversion various neutral polyazulenes to their polaron midgap states. Our model assumes that the polaron region of three azulene units is approximately coplanar (has almost zero dihedral angle) and that the infinitely extended polymer chain on either side of the polaron region have dihedral angles approaching those given in Table 2 that are characteristic of the corresponding biazulenes. The first (lower) polaron energy level is given by the HOMO energy of the corresponding triazulene (Table 3). This energy level is half filled as in Fig. 14. The second (upper) polaron energy level is given by corresponding LUMO and is empty. If this more coplanar ($\varphi \approx 0^\circ$) triazulene polaron was allowed to become indefinitely extended, then the first polaron energy level would approach that of corresponding coplanar polyazulene. Since polarons having an indeterminant number of azulene units with smaller dihedral angles, they must have HOMO values that range between these two extreme values, both are listed in Figures 17–20.

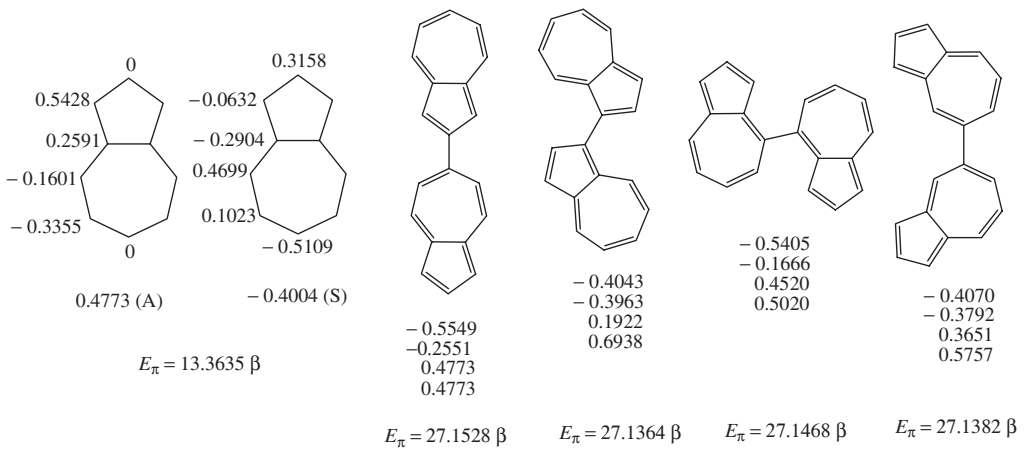

Figure 16. HOMO – LUMO eigenvalues/eigenvectors of azulene and eigenvalues of planar 2,6′-, 1,1′-, 4,4′-, 5,5′-biazulenes

DOI: 10.1002/poc

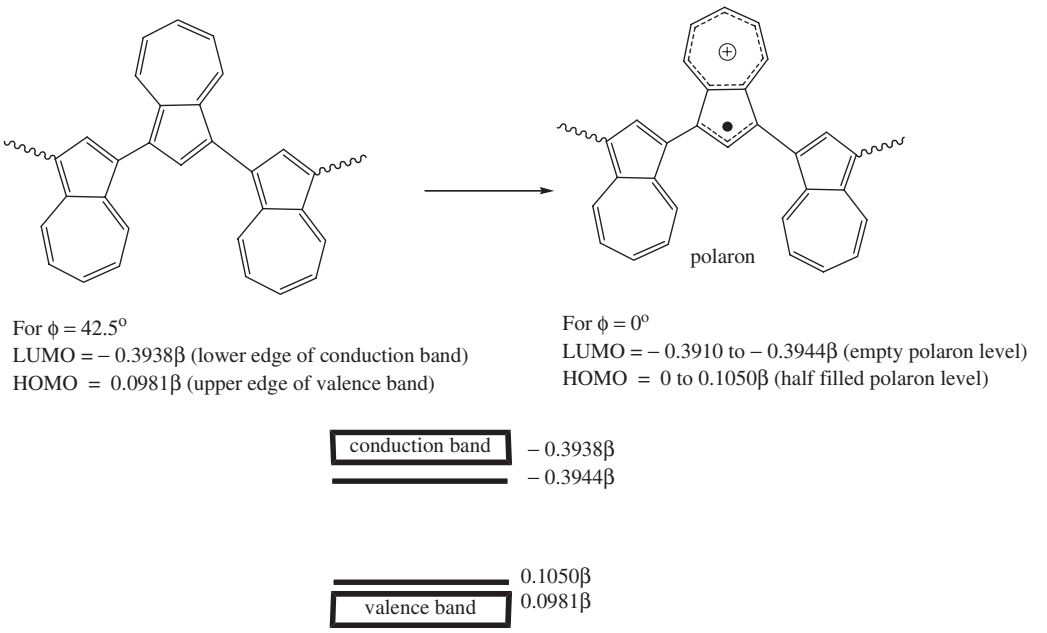

Figure 17. Formation of a polaron region within 1,3-polyazulene of infinite extent

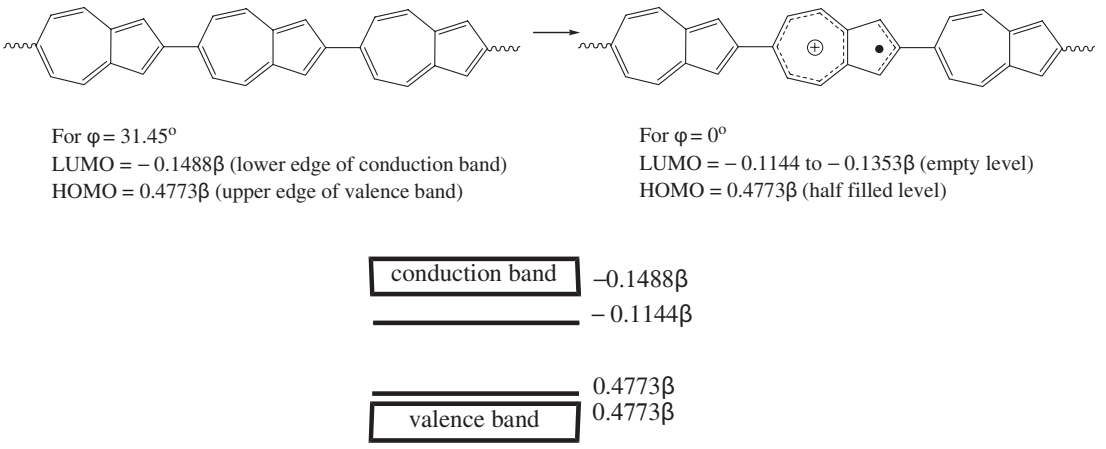

Figure 18. Formation of a polaron region within 2,6-polyazulene of infinite extent

The removal of an electron from the HOMO of the 1,3-polyazulene to form a polaron region of three azulene units which is composed of two azulenes, an allyl-like radical, and a positively charged tropylium (Fig. 17). This model corresponds exactly to the conclusion which suggested that positive net charges of the oxidized states are mainly localized in the seven membered rings and that in the polaron state the charge and spin parts are in separate rings of azulene unit of 1,3-polyazulene.[6,7] This result gives for the 1,3-polyazulene a first polaron energy level that is close to HOMO $= 0.1050\beta$ which overlaps with the valence band that is close to HOMO $= 0.0981\beta$ of the adjacent infinite twisted 1,3-polyazulene chains on either side leading to polaron conduction under the influence of electrical potential. In agreement with experiment,[6,7] it is predicted that 1,3-polyazulene should be capable of being made conductive by the polaron mechanism by oxidative doping.

Similarly, the removal of an electron from the valence band of the 2,6-polyazulene will form a polaron region of three azulene units (Fig. 18) with a first polaron energy level (HOMO $= 0.4773\beta$) that coincides with the valence band (HOMO $= 0.4773\beta$) of the adjacent infinite twisted 2,6-polyazulene chains on either side. Since the HOMO coefficients is zero for the 2,6-positions of azulene (Fig. 16), to the first approximation the HOMO splitting for 2,6'-biazulene is zero (Fig. 15). This results in the HOMO of 2,6-polyazulene being unchanged regardless of the dihedral angle or the number of its monomeric units. Thus, it is predicted that 2,6-polyazulene should be also

DOI: 10.1002/poc

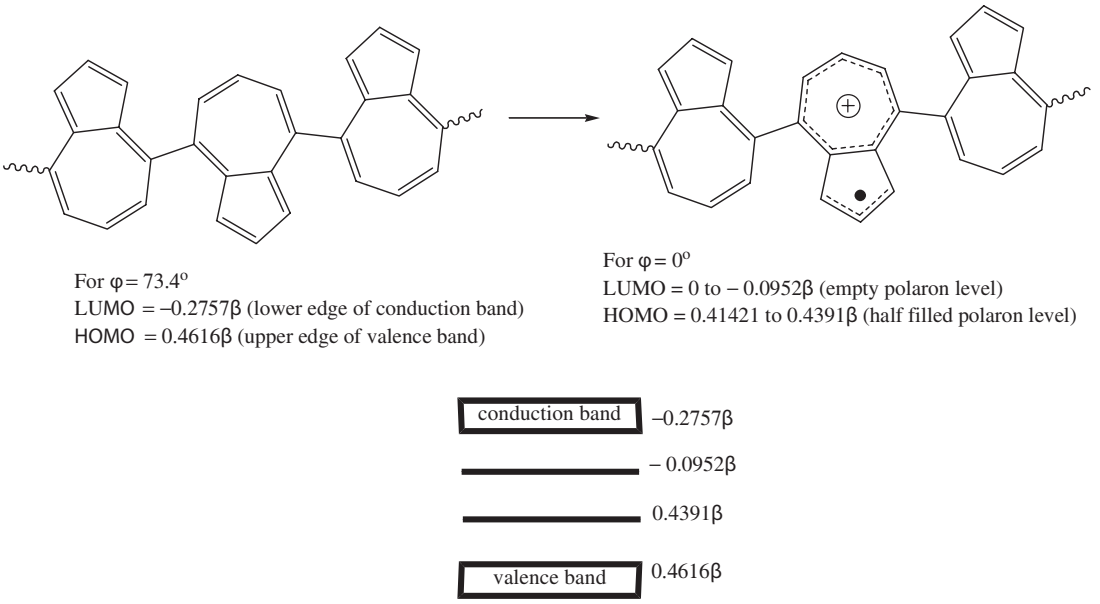

Figure 19. Formation of a polaron region within 4,8-polyazulene of infinite extent

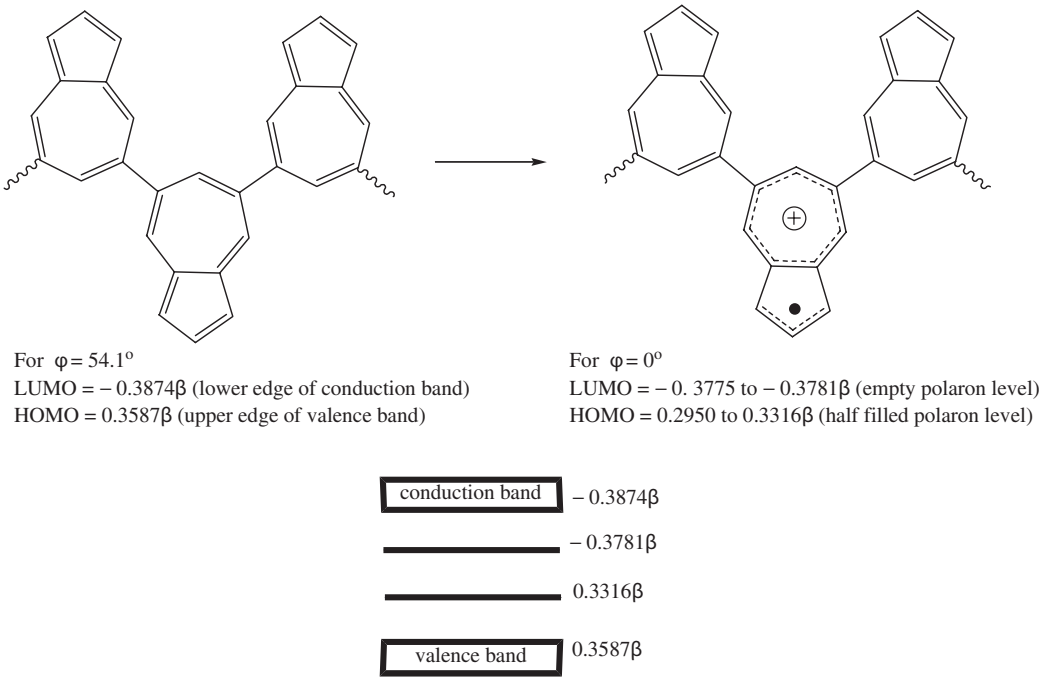

Figure 20. Formation of a polaron region within 5,7-polyazulene of infinite extent

capable of being made conductive by the polaron mechanism.

The removal of an electron from the HOMO of the 4,8-polyazulene (Fig. 19) or 5,7-polyazulene (Fig. 20) is expected to form a polaron region of three azulene units. The first (lower) polaron energy level is given by the HOMO energy of the corresponding triazulene which is half filled. The second (upper) polaron energy level is given by corresponding LUMO and is empty. The triazulenene first polaron energy levels for 4,8-polyazulene and 5,7-triazulene have values of HOMO = 0.4391 and 0.4391β, respectively, which are above the corresponding HOMO = 0.4616 and 0.3587β for their twisted infinitely extended systems. Thus, there exists a small gap (0.4616–0.391β and 0.3581–0.3316β) between the first polaron energy levels and the valence

DOI: 10.1002/poc

Table 3. HOMO – LUMO of planar terazulenes

Triazulene	HOMO (β)	LUMO (β)
2,6-	0.4773	−0.1353
1,3-	0.1050	−0.3944
4,8-	0.4391	−0.0.952
5,7-	0.3316	−0.3781

bands of the extended polymer branches, and we predict that polaron conduction for the 4,8- and 5,7- polyazulenes to be more difficult than for 1,3- and 2,6-polyazulenes. If these more coplanar ($\varphi = 0^\circ$) triazulene polaron regions are allowed to become infinitely extended, then the first polaron energy level increases to that of corresponding coplanar polyazulene, that is, from 0.4391 to 0.41421 and from 0.3316 to 0.2950β, respectively, and the respective gaps will increase.

In summary, our model for polaron conduction in polyazulenes deduces from MO symmetry that the polaron region is almost coplanar and is delocalized over approximately 3 azulene units. This hypothetical limit allows us to estimate the polaron midgap energy levels from the HOMO – LUMO of the corresponding triazulenes. This presupposes that conjugative interaction with the twisted polyazulene branches is only a small perturbation. That this is a reasonable model is corroborated by allowing the polaron region to hypothetically expand to infinity while still being bounded by infinite twisted polyazulene branches. Since the density of states is independent of boundary conditions, this sets the upper hypothetical limit for the first polaron energy level to that of the corresponding coplanar infinite polyazulenes. Along a similar line of reasoning, we predict that 1,3-polyazulene will be more easily made conducting by a polaron mechanism than the 2,6-, 4,8-, and 5,7-polyazulenes by reductive doping.

CONCLUSIONS

The polyazulenes of this study have significant gaps between the valence band and conduction band and are not expected to be intrinsically conductive. However, they can be made conductive via doping where the conduction mechanism is via polaron movement under the application of electrical potential because the gap between the valence band and the first polaron energy level is much smaller. It is predicted that the 1,3- and 2,6-polyazulenes will be more conductive by *p*-doping than the 4,8- and 5,7-polyazulenes. The predicted conduction of 1,3-polyazulene via the polaron mechanism is in agreement with experimental results.[6] HMO, MM2, and symmetry calculations of biazulenes and triazulenes were exploited in the analysis and modeling of the potential conductivity of polyazulenes.

REFERENCES

1. Michl J, Thulstrup EW. Why is Azulene Blue and Anthracene White? A Simple MO Picture. *Tetrahedron* 1976; **32**: 205–209.
2. Dias JR. Valence-Bond and Hückel Molecular Orbitals Diradicals – Alternant versus Nonalternant Effects. *Aust. J. Chem.* 2003; **56**: 1225–1232.
3. Morita T, Takase K. Synthesis of 1,1'-, 1,2'-,and 2,6'-Biazulene and Their Derivatives by Ullmann Reaction. *Bull. Chem. Soc. Jpn.* 1982; **55**: 1144–1154.
4. Hunig S, Ort B, Hanke M, Jutz C, Morita T, Takase K, Fukazawa Y, Aoyagi M, Ito S. Isomers of Biazulene: UV/VIS-Spectroscopy, Voltammetric, and HMO- Energies. *Liebigs. Ann. Chem.* 1984; 1952–1958.
5. Iyoda M, Sato K, Oda M. Nickel-Catalyzed Coupling of 1,6-Methano[10]annulene and Azulene. A facile synthesis of bi-, ter-, quarter-, and polyazulenes. *Tetrahedron Lett.* 1985; **26**: 3829–3832.
6. Wang F, Lai Y-H, Kocherginsky NM, Kosteski YY. The First Fully Characterized 1,3-Polyazulene. *Org. Lett.* 2003; **5**: 995–998.
7. Tanaka K, Toriumi M, Wang S, Yamabe T. Electronic Structure of Polyazulene. *Polymer J.* 1990; **22**: 1001–1006.
8. (a) McClelland BJ. Graphical Method for Factorizing Secular determinants of Huckel Molecular Orbital Theory. *J. Chem. Soc. Faraday Soc. Trans. II* 1974; **70**: 1453–1456; (b) McClelland BJ. Eigenvalues of the Topological Matrix. *J. Chem. Soc. Faraday Trans. 2* 1982; **78**: 911–916.; (c) McClelland BJ. On the Factorization of Huckel Characteristic Equations. *Molec. Phys.* 1982; **45**: 189–190.
9. (a) Dias , JR. Structural Origin of Specific Eigenvalues in Chemical Graphs of Planar Molecules. *Molec Phys.* 1995, **85**, 1043–1060; (b) Dias JR. Facile Determination of Molecular Graph Eigenvalues with Symmetrical Eigenvectors. *MATCH (Commun. Math. Comput. Chem.)* 2003; **48**: 55–61.
10. Hosoya H, Aida M, Kumagai R, Watanabe K. Analysis of the π–Electronic Structure of Infinitely Large Networks. *J. Comput. Chem.* 1987; **8**: 358–366.
11. Ledermann W. Asymptotic Formulae Relating to the Physical Theory of Crystals. *Proc. Roy. Soc.* 1944; **A182**: 362–377.
12. Gao Y-D, Kumazaki H, Terai J, Chida K, Hosoya H. Topological Factors Governing the HOMO-LUMO Band Gap of the Density of States of Periodic Hydrocarbon Polymer Networks. *J. Math. Chem.* 1993; **12**: 279–308.
13. Dias JR. *Molecular Orbital Calculations Using Chemical Graph Theory.* Springer-Verlag: Berlin, 1993.
14. Imamura A, Orimoto Y, Aoki Y. Molecular and Electronic Structures of Bipolaron in Poly-para-phenylene in Terms of Molecular Orbital symmetry. *Theor. Chem. Acc.* 1999; **102**: 180–187.
15. Mercouri MG. Conductive Polymers. *C&EN* 1990; Dec. 3, **68**: 36–54.

DOI: 10.1002/poc